Tr. J. of Engineering and Environmental Science
23 (1999) , 349 – 361.

A Panel Method for the Potential Flow Around 2-D Hydrofoils

Şakir BAL
Istanbul Technical University, Department of Naval Architecture,
80626, Maslak, Istanbul-TURKEY

Received 20.05.1997

Abstract

A potential-based panel method for the hydrodynamic analysis of 2-D hydrofoils moving under a free surface with constant speed without consideration of the cavitation phenomenon is described. By applying Green's theorem and choosing the value of internal potential as equal to the incoming flow potential, an integral equation for the total potential is obtained under the potential flow theory. The free surface condition is linearized and the Dirichlet boundary condition is used instead of the Neumann boundary condition. The 2-D hydrofoil is approximated by line panels on which there are only constant doublet distributions. The method of images is used for satisfying the linearized free surface condition and all the terms in the fundamental solution of total potential are integrated over a line panel. Pressure distribution, lift, wave resistance and free surface deformations are calculated for NACA4412, van de Vooren hydrofoils and a thin hydrofoil. Values obtained are higher than those in the literature, not only for the pressure distributions but also for the lift and wave resistance coefficients and wave elevations. The effect of free surface is examined by a parametric variation of the Froude number and depth of submergence.

Key Words: Potential Flow, 2D Hydrofoils, Free Surface.

İki Boyutlu Hidrofillerin Etrafındaki Potansiyel Akımın Hesabı için Bir Panel Yöntemi

Özet

Bu çalışmada, serbest su yüzeyinin altında, kavitasyon özelliği gözönüne alınmaksızın, sabit bir hızla ilerleyen iki boyutlu hidrofoillerin hidrodinamik analizi için potansiyel temelli bir panel yöntemi sunulmuştur. Green teoremini kullanarak ve dahili (iç) potansiyeli gelen düzgün akımın potansiyeline eşitleyerek, potansiyel akım teorisi koşulları altında toplam potansiyel için bir integral denklem oluşturulmuştur. Serbest su yüzeyi koşulu lineerleştirilmiş ve hidrofil üzerinde Neumann türü sınır koşulu yerine Dirichlet türü sınır koşulu kullanılmıştır. Hidrofoil, üzerinde sabit dağılımlı duble olan doğrusal panellere bölünmüştür. Serbest su yüzeyi koşulunu sağlamak için ayna simetriği yöntemi kullanılmış ve temel çözümdeki terimler her bir panel üzerinde integre edilmiştir. NACA4412, Van de Vooren hidrofoilleri ve ince bir hidrofil için basınç dağılımı, kaldırma kuvveti, dalga direnci ve serbest su yüzeyindeki deformasyonlar hesaplanmıştır. Literatürde var olan değerlerden (basınç dağılımı, kaldırma kuvveti, dalga direnci, serbest su yüzeyi deformasyonlarından) daha büyük değerler elde edilmiştir. Serbest su yüzeyinin hidrofoil üzerindeki etkisi Froude sayısına ve hidrofoil batma derinliğine bağlı olarak incelenmiştir.

Anahtar Sözcükler: Potansiyel Akım, İki Boyutlu Hidrofoiller, Serbest Su Yüzeyi.

Introduction

The practical importance of hydrodynamic analysis of 2-D hydrofoils moving under a free surface is very well-known. The results of the methods for 2-D hydrofoils offer comparison with similar results of the methods for 3-D hydrofoils. A 2-D analysis is also much faster than the corresponding 3-D analysis. Much attention has been given to this problem in recent literature.

In early years, thin-foil approximation and the Neumann boundary condition were generally used. Studies by Hough and Moran (1969) and Plotkin (1975) involved thin-foil approximation with linearized free surface condition. The former examined the flow around flat-plate and cambered-arc hydrofoils while the latter included a thickness correction around the leading edge. Giesing and Smith (1967), Bai (1978) and Yeung and Bouger (1979) dealt with thick-foil methods which provided much precise representation of the flow near the hydrofoil surface. Giesing and Smith (1967) distributed the Kelvin wave source on the hydrofoil surface, which satisfies the linearized free surface condition, and they obtained an integral equation for the source strength by applying the kinematic body boundary condition (the Neumann condition). This integral equation was solved numerically. Bai (1978) applied the localized finite-element numerical technique using Galerkin's method. In this method, an integral equation on the hydrofoil surface is replaced by a system of equations, over a much larger fluid domain but having a much simpler kernel. Yeung and Bouger (1979) used a hybrid integral equation method based on Green's theorem. They satisfied the linearized free surface condition and the exact body condition.

In addition, Salvesen (1969), Kennell and Plotkin (1984), Forbes (1985) and Bai and Han (1994) computed nonlinear free-surface effects. Salvesen (1969) derived a consistent second-order perturbation theory. Kennell and Plotkin (1984) also computed the second-order effects of the free surface for thin-hydrofoils. They provided consistent approximation to the flow properties both on the hydrofoil surface and on the free surface. Forbes (1985) satisfied the fully nonlinear free surface condition. Bai and Han (1994) applied the localized finite-element method to solve the nonlinear problem. Wu and Eatock Taylor (1995) compared the finite element method with the boundary element method for the nonlinear time stepping solution of 2-D hydrofoils. Such nonlinearities are not included in this study. However, the present method can be used as the first step for a systematic iterative procedure for solving the fully nonlinear problem.

In this study, a constant potential-based panel method (Dirichlet boundary condition), which is explained in detail in Katz and Plotkin (1991) and Moran (1984), is applied to the 2-D hydrofoils moving under a free surface. By applying Green's theorem and choosing the internal potential as a negative of the incoming velocity potential, an integral equation for the total potential is obtained. Discretization of this integral equation gives a panel method which Kerwin *et al.* (1987) call the total potential method. The method of images is used to consider the linearized free surface condition. A numerical technique expressed in Giesing and Smith (1967) is used in the fundamental solution (Green function) of the total velocity potential. The method is first applied to NACA4412 hydrofoil in order to compare the results with those in the literature. Pressure distribution, lift, wave resistance and free surface deformation are given for different submergence/chord ratios and different Froude numbers. Values obtained for pressure, lift and wave resistance coefficients are higher than those in the literature. Next, the method is applied to van de Vooren hydrofoil for additional results. The effect of the submergence depth of the hydrofoil from the free surface and the Froude number on the lift and wave resistance coefficients is examined by a parametric study. As a last example, a thin hydrofoil with an elliptic nose and trailing edge and a NACA 1.75-65 mean-line camber is chosen in order to compare the experimental lift values with those obtained by this method. Details of this hydrofoil can be found in Giesing and Smith (1967).

1. Mathematical Formulation

Consider a steady uniform flow past a fixed 2-D hydrofoil under the free surface of a fluid. The Oxz cartesian coordinate system is chosen, as shown in Figure 1. It is assumed that the fluid is incompressible, inviscid and that the flow is irrotational. Thus, the steady 2-D flow can be described by a total potential as follows:

$$\Phi(x,z) = Ux + \phi(x,z) \tag{1}$$

where U is the incoming uniform flow velocity and ϕ is the perturbation velocity potential which must satisfy the Laplace equation in domain D,

$$\nabla^2\phi(x,z) = 0 \tag{2}$$

The corresponding boundary value problem can now be constructed by specifying boundary conditions on the total boundary $S(S = S_H \bigcup S_W \bigcup S_F \bigcup S_I \bigcup S_B)$ as follows:

The kinematic body boundary condition should be satisfied on S_H :

$$\frac{\partial\phi}{\partial n} = -\vec{U}.\vec{n} \tag{3}$$

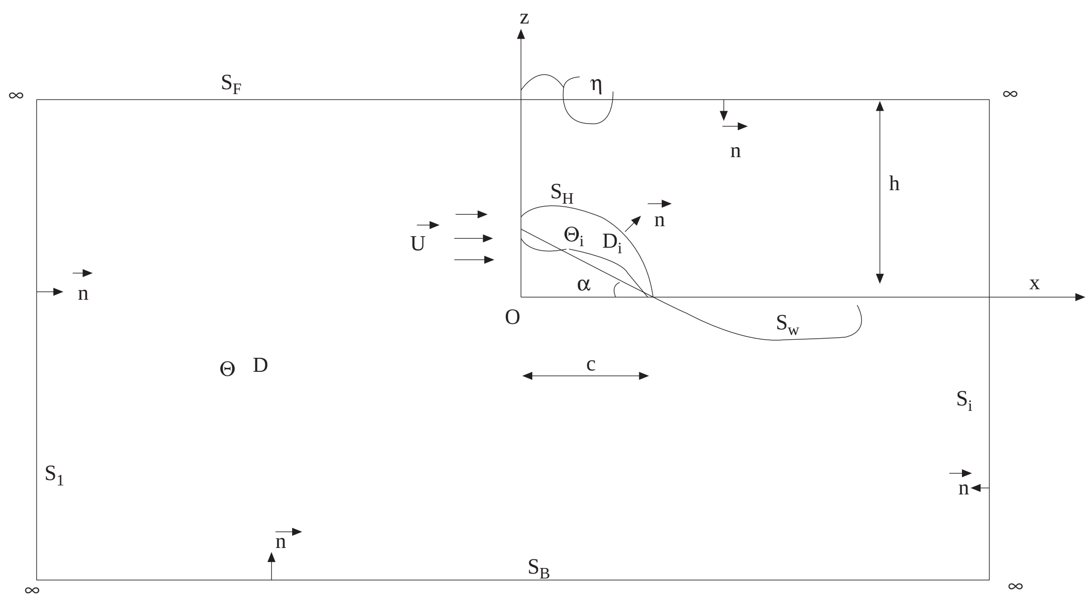

Figure 1. Definition of coordinate system and notations.

The kinematic and dynamic (Bernoulli equation on the free surface) free surface conditions should be satisfied on S_F:

$$\frac{D\eta}{Dt} = 0 \tag{4a}$$

$$\frac{P_A}{\rho} + \frac{1}{2}U^2 = \frac{P_A}{\rho} + \frac{1}{2}V^2 + g\eta \tag{4b}$$

where $\frac{D}{Dt} = \frac{\partial}{\partial t} + \vec{v}.\vec{\nabla}$ is the material derivative, P_A is the atmospheric pressure, V is the total velocity and η is the free surface deformation. By combining the kinematic and dynamic free surface conditions and linearizing the resulting equation, the following free surface equation can be obtained:

$$\phi_{xx}(x,h) + k_0\phi_z(x,h) = 0 \tag{5}$$

where $k_0 = g/U^2$ (g: gravitational acceleration).

A Kutta condition should be satisfied at the trailing edge:

$$P_{TE^+} = P_{TE^-} \tag{6}$$

where P_{TE^-} indicate the pressure values at the upper and lower side of the trailing edge, respectively.

The wake surface has zero thickness and the pressure jump across S_w is zero, while there is a jump in the potential:

$$\Delta P = P^+ - P^- = 0 \tag{7}$$

$$\Delta\phi = \phi^+ - \phi^- = \Gamma \tag{8}$$

where ΔP are $\Delta\phi$ are the pressure and potential jump on the S_w, respectively, and the constant Γ is the circulation around the body, which should be determined as a part of the solution.

The bottom condition for infinite depth (on S_B) is:

$$lim_{z\to-\infty}\nabla\phi(x,z) = 0 \tag{9}$$

No disturbances exist for far upstream, while the potential is bounded for far downstream as a radiation condition:

$$lim_{x\to-\infty}|\nabla\phi| \to 0 \tag{10a}$$

$$lim_{x \to -\infty} \phi \leq \infty \tag{10b}$$

The boundary value problem defined above can be transformed into an integral equation by applying Green's theorem to bounday S and assuming a fictitious internal fluid in D_i, as also indicated in Lamb (1932) and Katz and Plotkin (1991), as follows:

$$\int_S \left\{ [\phi(q) - \phi_i(q)] \frac{\partial}{\partial n_q} G(p;q) - \left[\frac{\partial \phi(q)}{\partial n_q} - \frac{\partial \phi_i(q)}{\partial n_q} \right] G(p;q) \right\} dS(q) = 0 \tag{11}$$

where ϕ : perturbation velocity potential in D_i

ϕ_i : internal perturbation velocity potential in D_i

$p(x, z)$: field point where induced potential is calculated

$q(\xi, \zeta)$: source point where singularity is located

$\frac{\partial}{\partial n_q}$: normal derivative with respect to point q

$G(p; q)$: Green function of the problem

According to Lamb (1932), if $\partial\Phi/\partial n$ =0 for an enclosed boundary (here S), as required by the body boundary condition in equation (3), then the potential inside the body (without any singularities) will stay constant:

$$\phi_i = constant \tag{12}$$

This allows us to specify the body boundary condition in equation (3) indirectly, which is known as the Dirichlet boundary condition. ϕ_i can now be selected as a negative of the incoming velocity potential, that is, $\phi_i = -\phi_\infty(\nabla\phi_\infty = \vec{U})$. Thus, the second term in equation (11) becomes zero because of the body boundary condition in equation (3). The first term in equation (11), which is the difference between ϕ and ϕ_i, becomes the total potential:

$$\phi - \phi_i = \phi + \phi_\infty \equiv \Phi \tag{13}$$

Thus, equation (11) can be rewritten as follows:

$$\int_S \Phi(q) \frac{\partial}{\partial n_q} G(p;q) dS(q) = 0 \tag{14}$$

This means that there is a doublet distribution, which has the strength $\Phi(q)$, over the whole boundary S. It should also be noted that the singularity in equation (14) for $p \to q$ is not yet excluded from equation (14). The normal derivative of the Green function $G(p; q)$ (or the free-surface Green function of the doublet) which should satisfy equations (2), (4), (9) and (10a,b), can be obtained by the method of images, as follows (see Appendix):

$$\begin{aligned} \frac{\partial}{\partial n_q} G(p;q) = & -\frac{1}{2\pi} \frac{z-\zeta}{(x-\xi)^2 + (z-\zeta)^2} \\ & + \frac{1}{2\pi} \frac{2h - z + \zeta}{(x-\xi)^2 + (2h - z + \zeta)^2} \\ & + \frac{k_0}{\pi} \int_0^\infty \frac{e^{-k(2h-z+\zeta)} \cos k(x-\xi)}{k - k_0} dk \\ & -2k_0 e^{-k_0(2h-z+\zeta)} \sin k_0(x-\xi) \end{aligned} \tag{15}$$

Since the integral equation (14) for the Green function above automatically satisfies the free surface, the bottom and the radiation conditions on S_F, S_B and S_1, respectively, it can be concluded that the integral equation (14) can be written as follows:

$$\int_{S_H} \Phi(q) \frac{\partial}{\partial n_q} G(p;q) dS(q) + \int_{s_w} \Delta\Phi(q) \frac{\partial}{\partial n_q} G(p;q) dS(q) + \phi_\infty(p) = 0 \tag{16}$$

An integral equation similar to the one obtained above is given in Lee *et al.* (1994). This integral equation can be solved numerically, as explained below.

2. Numerical Procedure

In order to obtain an approximate solution for the integral equation (16), the hydrofoil surface is divided into N small line panels. The values $\Phi(q)$ are assumed to be constant within each panel. $\Delta\Phi(q)$ is assumed to be equal to the value at the trailing edge $(\Delta\Phi(q) = \Delta\Phi_{TE})$ by recalling the Kutta condition, equation (8). Then the collocation method is used, that is, equation (16) is satisfed at the centroids of each panel. This yields the following linear algebraic equation system:

$$\sum_{j=1}^{N} (C_{ij} + W_{ij}) \Phi_j = -\Phi_{\infty i} \quad ; i = 1, \ldots, N \tag{17}$$

where

$$C_{ij} = \int_{S_j} \frac{\partial G_{ij}}{\partial n_j} dS_j \tag{18a}$$

$$W_{ij} = \int_{S_j} \frac{\partial G_{ij}}{\partial n_j} dS_j \tag{18b}$$

For the panels not in contact with the trailing edge $W_{ij} = 0.S_j$, is the line of the wake emanating from the trailing edge and extending to the infinity on z=0. The first two terms in the influence coefficients of the constant doublet line panel (in C_{ij} and W_{ij}) can be evaluated analytically in the panel's frame of reference, as also given in Katz and Plotkin (1991) and Moran (1984), as follows:

$$\begin{aligned} C_{ij} = &-\frac{1}{2\pi}\left\{tan^{-1}\frac{z-\zeta}{x-\xi_2} - tan^{-1}\frac{z-\zeta}{x-\xi_1}\right\} \\ &+ \frac{1}{2\pi}\left\{tan^{-1}\frac{2h-z+\zeta}{x-\xi_2} - tan^{-1}\frac{2h-z+\zeta}{x-\xi_1}\right\} \\ &+ \frac{k_0}{\pi}\int_{\xi_1}^{\xi_2} d\xi \int_0^\infty \frac{e^{-k(2h-z+\zeta)}\cos k(x-\xi)}{k-k_0} dk \\ &-2k_0 \int_{\xi_1}^{\xi_2} e^{-k_0(2h-z+\zeta)} \sin k_0(x-\xi) d\xi \end{aligned} \tag{19}$$

Here, ξ_1 and ξ_2 are the coordinates of the end points of the line panel in the panel coordinate system. The values of W_{ij} are exactly the same for the C_{ij}'s so they are not written here again. For the last two terms in equation (19), the integration with respect to ξ is made so that:

$$\begin{aligned} C_{ij} = &-\frac{1}{2\pi}\left\{tan^{-1}\frac{z-\zeta}{x-\xi_2} - tan^{-1}\frac{z-\zeta}{x-\xi_1}\right\} \\ &+ \frac{1}{2\pi}\left\{tan^{-1}\frac{2h-z+\zeta}{x-\xi_2} - tan^{-1}\frac{2h-z+\zeta}{x-\xi_1}\right\} \\ &+ \frac{k_0}{\pi}\int_0^\infty \frac{e^{-k(2h-z+\zeta)}[\sin k(x-\xi_2) - \sin k(x-\xi_1)]}{k(k-k_0)} dk \\ &-2e^{-k_0(2h-z+\zeta)}[\cos k_0(x-\xi_2) - \cos k_0(x-\xi_1)] \end{aligned} \tag{20}$$

For the integration with respect to k in equation (20), the method proposed by Giesing and Smith (1967) is used (see Appendix).

By solving the linear algebraic equation system, equation (3.1), the strength of doublets Φ_j is obtained. Once the strength of doublets Φ_j is known, the local external tangential velocity on each collocation point can be calculated by differentiating the velocity potential along the tangential direction, as follows:

$$V_{t_j} = \frac{\Phi_{j+1} - \Phi_j}{\Delta l_j} \tag{21}$$

where Δl_j is the distance between two adjacent collocation points. The pressure coefficient can now be computed b using Bernoulli's equation such that:

$$C_{P_j} = \frac{P_j - p_\infty}{\frac{1}{2}\rho U^2} = 1 - (\frac{V_{t_j}}{U})^2 \tag{22}$$

where P_j and p_∞ are the pressure values at the jth collocation point and at infinity, respectively. ρ is the density of the fluid. The contribution to the lift and wave resistance coefficients is then:

$$C_{L_j} = -C_{p_j} n_{z_j} \tag{23}$$

$$C_{W_j} = -C_{p_j} n_{x_j} \tag{24}$$

where n_x and n_z are the x and z components of the unit normal vector on the jth collocation point. For the wave elevation on the free surface, the following equation can be derived from Bernoulli's equation (see eqn.(4b)):

$$\eta = -\frac{U}{g}\frac{\partial \Phi(p)}{\partial x}, z = h \tag{25}$$

where $\Phi(p)$ is the total potential on the free surface and $\frac{\partial \Phi(x,h)}{\partial x}$ can be calculated easily by using the same technique given in the Appendix.

3. Numerical Results

A number of numerical tests is done to verify the present numerical method. First, the NACA4412 hydrofoil with angle of attack $\alpha = 5°$ is chosen to compare the results with those in Yeung and Bouger (1979) and Giesing and Smith (1967). In Figure 2, the calculated pressure distirbution on the hydrofoil for $F_c = 1(F_c = U/(gc)^{0.5}$, the Froude number) and h/c=1 is compared with the one given in Yeung and Bouger (1979). The total number of panels (N) for this case is 90. The corresponding lift and wave resistance coefficient values are also added to Figure 2. The C_p values calculated by the present method are higher than those obtained by Yeung and Bouger's (1979). In Figures (3a,3b,3c), the wave elevations nondimensionilized by h are given for different Froude numbers and fixed submergence depth/chord (h/c=1) ratios as compared with those in Yeung and Bouger (1979). The nondimensionilized wave elevations are also higher than Yeung and Bouger's (1979) as an absolute value. In Figure 4, the effect of the Froude number on the lift coefficient is shown as compared with that given in Yeung and Bouger (1979). It can easily be seen that the free surface causes a decrease in the lift coefficient of the hydrofoil for increasing Froude numbers. Furthermore, for this hydrofoil, the values $F_c = 1.03$ and h/c=0.94 are chosen to compare the pressure distribution, lift and wave resistance coefficiens with the experimental ones given in Giesing and Smith (1967). The corresponding results are given in Figure 5. Higher values for pressure, lift and wave resistance were obtained. The most probable reason for this may be that the total velocity potential is used instead of the perturbation velocity potential in the calculations.

Second, a van de Vooren hydrofoil having a thickness parameter of $\epsilon = 0.15$ and a trailing edge angle of $\tau = 10°$ is chosen (see Katz and Plotkin (1991) for details). The angle of attack was $\alpha = 5°$ and the total number of panels on the hydrofoil surface is N=90. The effect of the Froude number and h/c ratios is examined for this hydrofoil. In Figure 6 and Figure 7, the effects of h/c ratios on $C_L/C_{L\infty}$ and C_W values for $F_c = 1$ are given, respectively. Here, $C_{L\infty}$ is the lift coefficient of the hydrofoil in an unbounded fluid. It is found that for fixed Froude number, if the hydrofoil approaches the free surface, the lift value decreases and the wave resistance value increases. In Figure 8 and Figure 9, the effects of the Froude number on $C_L/C_{L\infty}$ and C_W for h/c=1 are given, respectively. It is found that for a fixed h/c ratio and an increasing Froude number, both the lift and wave resistance values decrease.

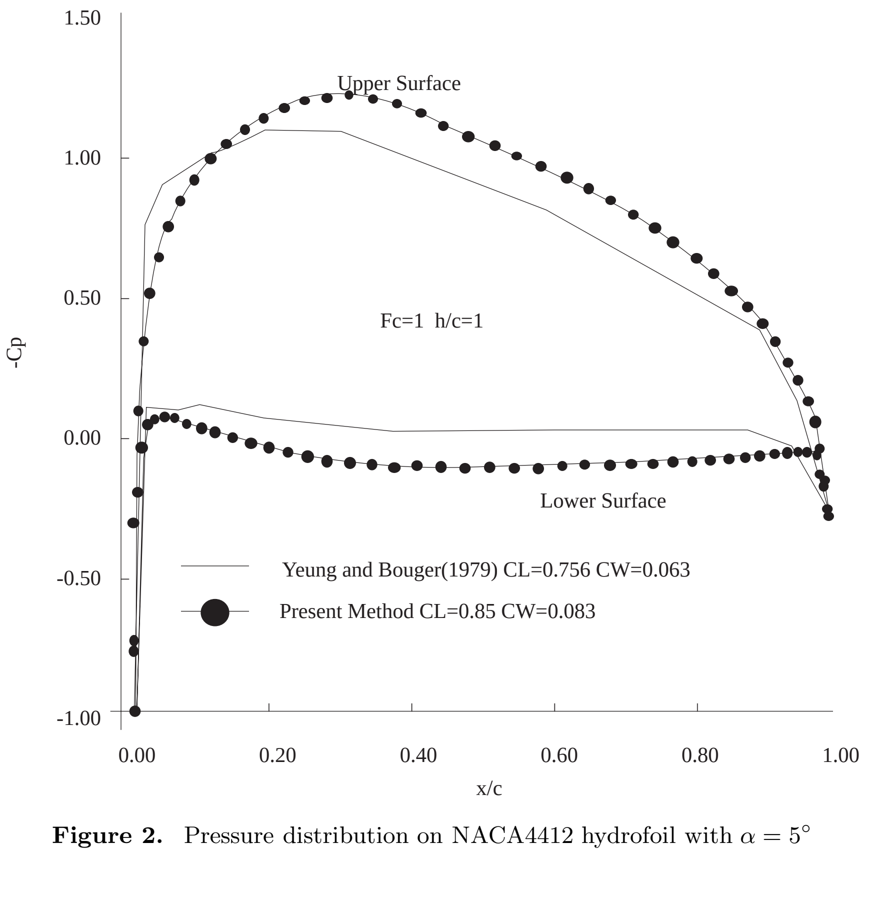

Figure 2. Pressure distribution on NACA4412 hydrofoil with $\alpha = 5°$

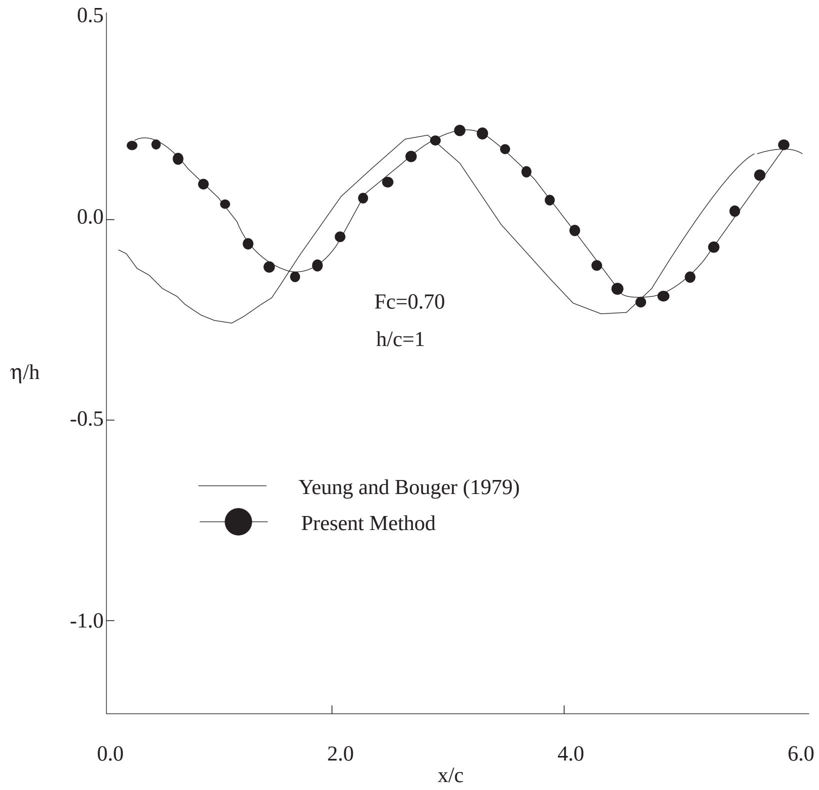

Figure 3a. Wave eleveations of NACA4412 hydrofoil with $\alpha = 5°$.

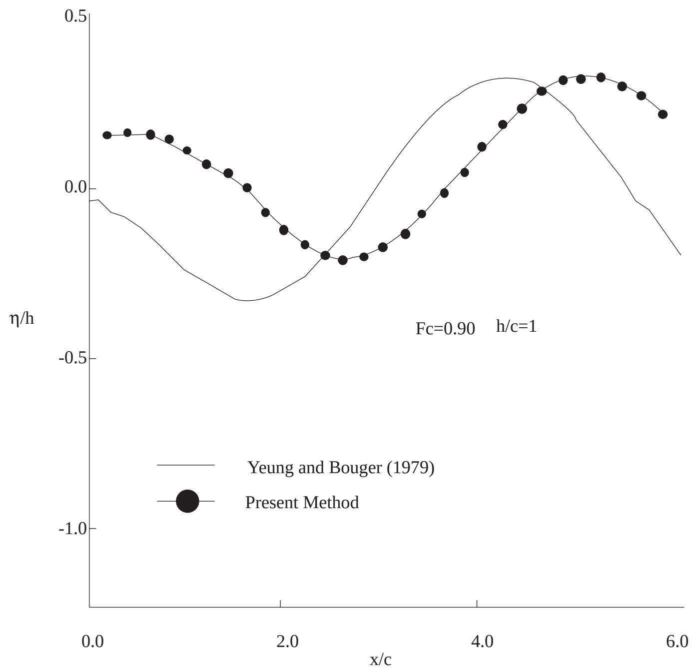

Figure 3b. Wave eleveations of NACA4412 hydrofoil with $\alpha = 5°$.

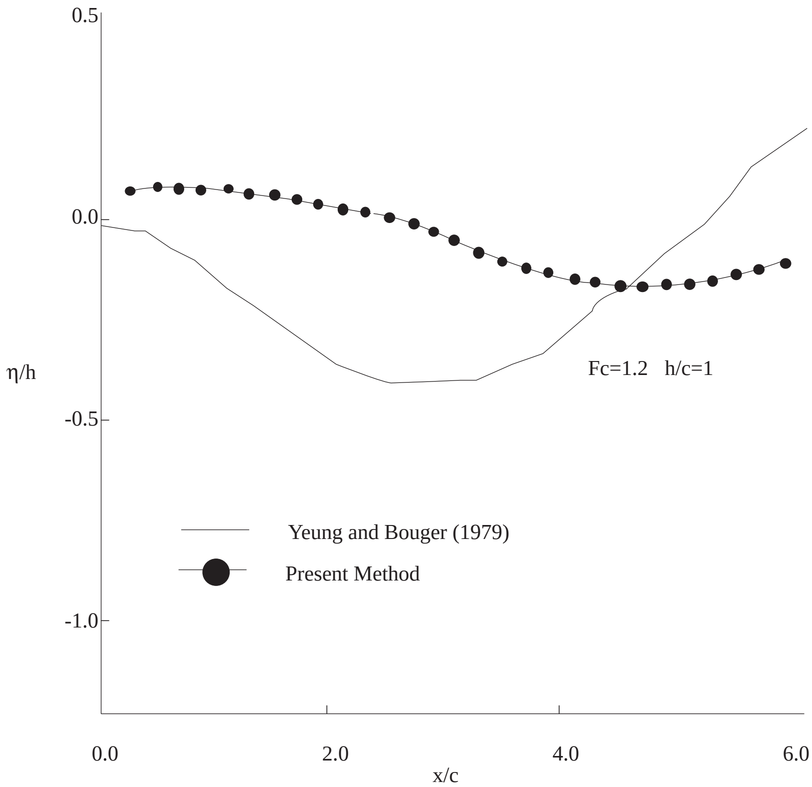

Figure 3c. Wave eleveations of NACA4412 hydrofoil with $\alpha = 5^{\circ}$.

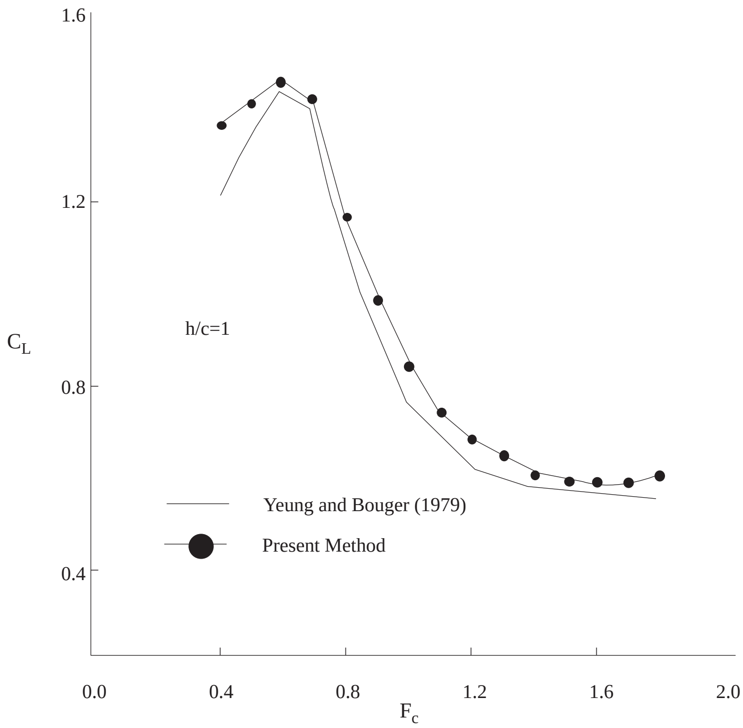

Figure 4. Lift coefficient of NACA4412 hydrofoil with $\alpha = 5^{\circ}$ for increasing Froude number.

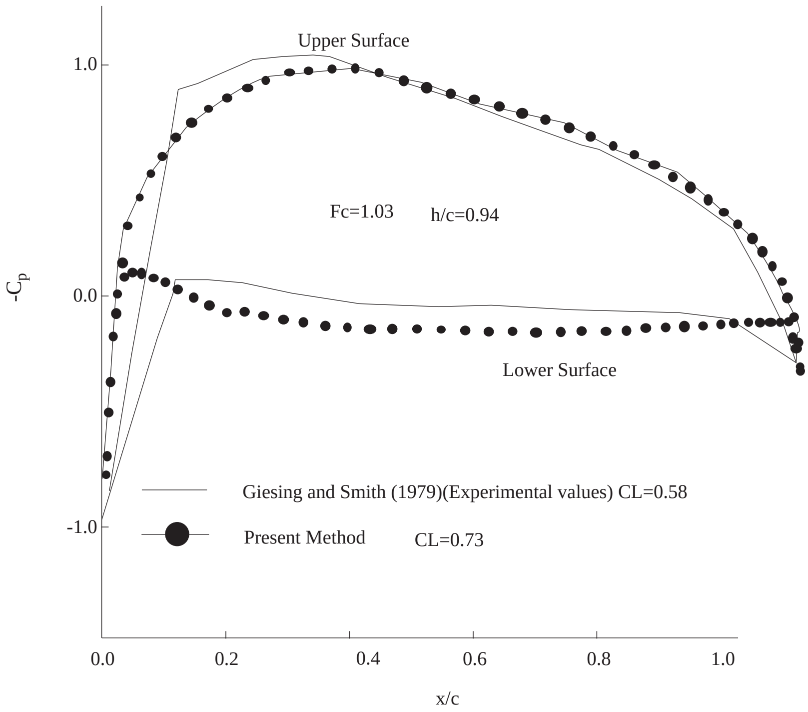

Figure 5. Pressure distribution on NACA4412 hydrofoil with $\alpha = 5°$.

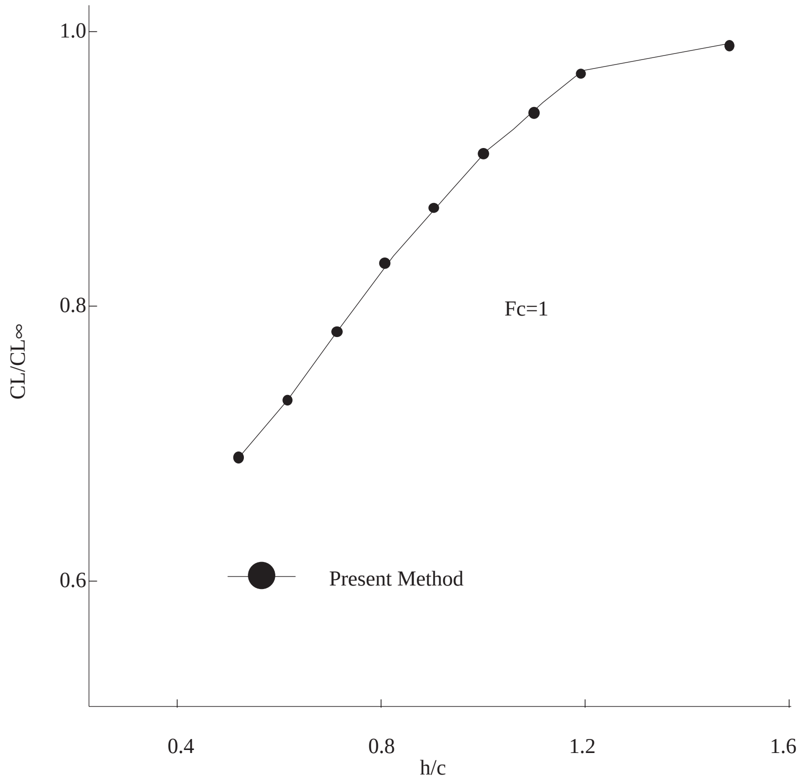

Figure 6. Variation of lift coefficient of van de Vooren hydrofoil with $\alpha = 5°$ for increasing h/c ratios.

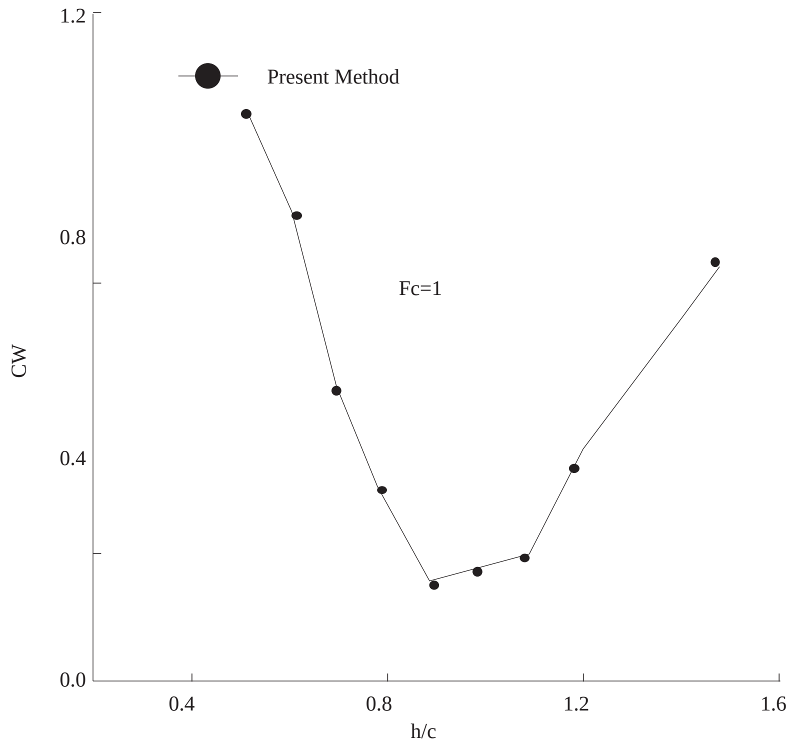

Figure 7. Variation of wave resistance coefficient of van de Vooren hydrofoil with $\alpha = 5^{\circ}$ for increasing h/c ratios.

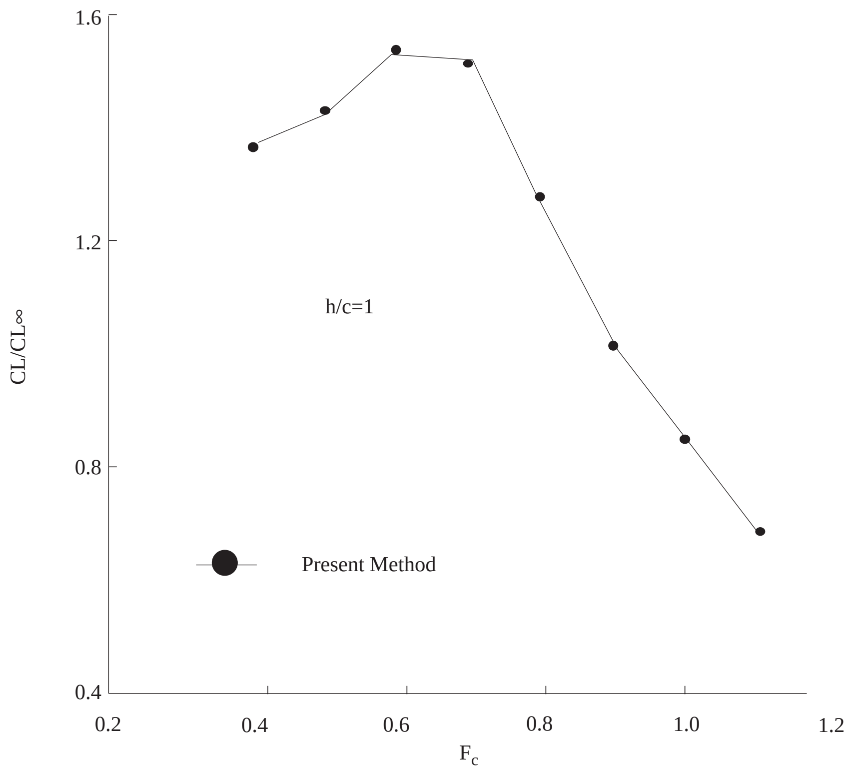

Figure 8. Variation of lift coefficient of van de Vooren hydrofoil with $\alpha = 5^{\circ}$ for increasing Froude number.

Third, a thin hydrofoil with an elliptic nose and trailing edge and an NACA 1.75-65 meanline camber is chosen. The thickness ratio is 3% and the details of this hydrofoil are given in Giesing and Smith (1967). The angle of attack is $\alpha = 0°$ and the total number of panels on the hydrofoil surface is N=90. Experimental lift coefficient values (C_L) are equal to 0.206 for h/c=1, F_c=1.414 and to 0.273 for h/c=2, F_c=2, respectively. The C_L calculated values by the present method are 0.223 and 0.280, respectively. The lift coefficient values obtained are higher than the experimental ones.

4. Conclusions

In this study, a constant potential-based panel method for the steady flow of a 2-D hydrofoil under a free surface is presented. An integral equation derived from Green's theorem is approximated by dividing the hydrofoil surface into small line panels. The influence coefficients are calculated analytically in the near field. The numerical approximation given in Giesing and Smith (1967) is used in evaluating the doublet wave terms in the Green function. The results (pressure distribution, lift and wave resistance coefficients and wave elevations on the free surface) obtained by the present method are higher than those in the literature. The main reason for this may be that the total velocity potential is used rather than the perturbation velocity potential in equation (16).

The negative effects of the free surface on the lift and wave resistance coefficients are shown for an increasing Froude number and decreasing h/c ratios. The free surface is found to cause a decrease in the lift coefficient of the hydrofoil for higher Froude numbers and an increase in the wave resistance coefficient of the hydrofoil for smaller h/c ratios. This method can also be extended to include the cavitation characteristics of the hydrofoil. This is now under investigation.

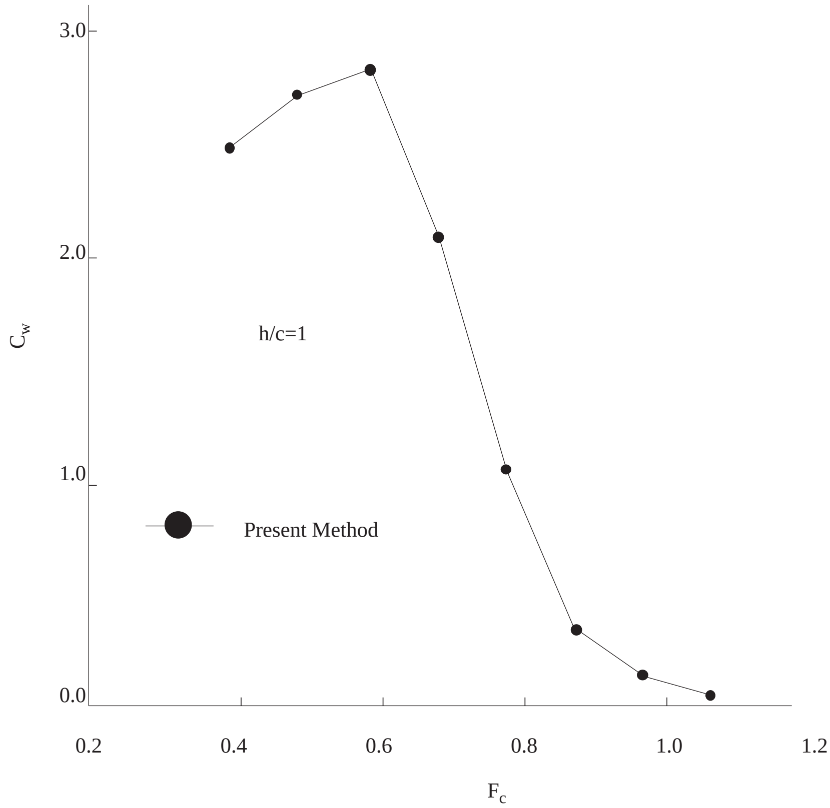

Figure 9. Variation of wave resistance coefficient of van de Vooren hydrofoil with $\alpha = 5°$ for increasing Froude number.

5. Acknowledgments

The author wishes to express his gratitude to Professors T. Sabuncu and A.Y. Odabası of the Department of Naval Architecture of Istanbul Technical University.

6. List of Symbols

c	=	Chord of hydrofoil
C_{ij}	=	Influence coefficient of doublet line panel
C_L	=	Lift coefficient
C_P	=	Pressure coefficient
C_W	=	Wave resistance coefficient
D	=	Fluid domain outside the hydrofoil
D_i	=	Inside domain of the hydrofoil
D/Dt	=	Material derivative
F_c	=	Froude number
g	=	Gravitational acceleration
G(p;q)	=	Green function
h	=	The submergence of the hydrofoil from free surface
$n(n_x, n_z)$	=	Unit normal vector
N	=	Total number of panels
p_i	=	Pressure value on the ith panel
S	=	Total boundary surface of the fluid domain
S_H	=	Hydrofoil surface
S_W	=	Wake surface
S_F	=	Free surface
S_I	=	The surfaces at infinity
S_B	=	Bottom surface
$\vec{U}$	=	The velocity of incoming uniform flow
$\vec{V}$	=	Total velocity vector
W_{ij}	=	Influence coefficient of wake
α	=	Angle of attack
Γ	=	Circulation value
ρ	=	Density of water
ϕ	=	Perturbation velocity potential
Φ	=	Total velocity potential
η	=	Wave elevations on the free surface
$\vec{\nabla}$	=	Gradient operator

7. Appendix: Calculation of Free Surface Green Function for a Point Doublet

The Green function of a point doublet in an unbounded fluid can be written as follows (see Katz and Plotkin (1991) and Moran (1984)):

$$\frac{\partial}{\partial n_q} G(x, z; \xi, \zeta) = -\frac{1}{2\pi} \frac{z-\zeta}{(x-\xi)^2 + (z-\zeta)^2} \tag{1a}$$

By using the integral equation given below,

$$\int_0^\infty e^{-k|z|} \cos kx dk = \frac{|z|}{x^2 + z^2} \tag{1b}$$

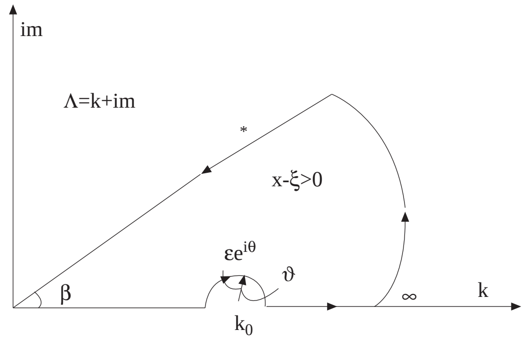

Figure A1.

and considering that the Green function should satisfy the free surface condition, equation (5), the following equation can be written for the Green function:

$$\frac{\partial}{\partial n_q} G(x, z; \xi, \zeta) = -\frac{1}{2\pi} \int_0^\infty e^{-k(z-\zeta)} \cos k(x-\xi) dk + \frac{1}{2\pi} \int_0^\infty e^{k(z-\zeta)} \cos k(x-\xi) A(k) dk \tag{1c}$$

where A(k) should be determined by the free surface condition. A(k) can be calculated as follows:

$$A(k) = e^{-2kh}\left(1 + \frac{2k_0}{k-k_0}\right) \tag{1d}$$

Thus, the normal derivative of the Green function by the method of images becomes

$$\frac{\partial}{\partial n_q} G(x, z; \xi, \zeta) = -\frac{1}{2\pi} \frac{z-\zeta}{(x-\xi)^2 + (z-\zeta)^2} + \frac{1}{2\pi} \frac{2h - z + \zeta}{(x-\xi)^2 + (z-\zeta)^2} \tag{1e}$$

$$+\frac{k_0}{\pi} PV \int_0^\infty \frac{e^{-k(2h-z+\zeta)} \cos k(x-\xi)}{k-k_0} dk$$

where PV indicates the principal value of the integral. This principal value of the integral can be handled by using contour integration in the complex Λ-plane. To do this, the following complex integral is written on the contour given in Figure A1:

$$\oint_C \frac{e^{-\Lambda[(2h-z+\zeta)-i(x-\xi)]}}{\Lambda - k_0} d\Lambda \tag{1f}$$

where C is the contour defined in Figure A1. By using the Cauchy theorem, the following equation can be obtained:

$$PV \int_0^\infty \frac{e^{-k[(2h-z+\zeta)-i(x-\xi)]}}{k-k_0} dk = sgn(x-\xi) i\pi e^{-k_0[2h-z+\zeta-i(x-\xi)]} + \int_0^\infty \frac{e^{-k} dk}{k - k_0[2h-z+\zeta-i(x-\xi)]} \tag{2a}$$

It is possible to find angle α such that the term $e^{-k[2h-z+\zeta-i(x-\xi)]}$ is purely real along contour ($\star$) such that the oscillatory integrand for k>> 0 is prevented. Thus, it is found that:

$$\alpha = \tan^{-1}(\frac{x-\xi}{2h-z+\zeta}) \tag{3a}$$

See Giesing and Smith (1967) for details.

References

Bai, K.J., “A localized finite-element method for two-dimensional steady potential flows with a free surface”, Journal of Ship Research, Vo.22, pp.216-230, 1978.

Bai, K.J. and Han, J.H., “A localized finite-element method for the nonlinear steady waves due to a two-dimensional hydrofoil”, Journal of Ship Research, Vol.38, pp.42-51, 1994.

Forbes, L.K., “A numerical method for non-linear flow about a submerged hydrofoil”, Journal of Engineering Mathematics, Vol.19, pp.329-339, 1985.

Giesing, J.P. and Smith, A.M.O., “Potential flow about two-dimensional hydrofoils”, Journal of Fluid Mechanics, Vo.28, pp.113-129, 1967.

Hough, G.R. and Moran, S.P., “Froude number effects on two-dimensional hydrofoils”, Journal of Ship Research, Vol.13, pp.53-60, 1969.

Katz, J. and Plotkin, A., Low speed aerodynamics from wing theory to panel methods, McGraw-Hill Inc., New York, 1991.

Kennell, C. and Plotkin, A., “A second order theory for the potential flow about thin hydrofoils”, Journal of Ship Research, Vol.28, pp.55-64, 1984.

Kerwin, J.E., Kinnas, S.A., Lee, J.T. and Shih, W.Z., “A surface panel method for the hydrodynamic analysis of ducted propellers”, SNAME Trans., Vol.95, pp.93-122, 1987.

Lamb, H., Hydrodynamics, 6th ed. Dover Publications, 1932.

Lee, C.S., Lew, J.M. and Kim, Y.G., “Analysis of a two-dimensional partially or supercavitating hydrofoil advancing under a free surface with a finite froude number”, 20th Symposium of Naval Hydrodynamics, USA, 1994.

Moran, J., An introduction to theoretical and computational aerodynamics, John Wiley and Sons Inc., New York, 1984.

Plotkin, A., “Thin-hydrofoil thickness problem including leading-edge corrections”, Journal of Ship Research, Vol.19, pp.122-129, 1975.

Salvasen, N., “On higher-order wave theory for submerged two-dimensional bodies”, Journal of Fluid Mechanics, Vol.38, pp.415-432, 1969.

Wu, G.K. and Eatock Taylor, R., “Time stepping solutions of the two dimensional nonlinear wave radiation problem”, International Journal of Ocean Engineering, Vol.22, pp.785-798, 1995.

Yeung, R.W. and Bouger, Y.C., “A hybrid-integral equation method for steady two-dimensinal ship waves”, International Journal of Numerical Methods in Engineering, Vol.14, pp.317-336, 1979.